

Nonlinear dynamics with an RL-Diode Circuit

Fatima Perwaiz and Muhammad Sabieh Anwar

LUMS School of Science and Engineering

07-23-2019

Abstract

This experiment is based on Chaos theory and the nonlinear dynamics of an RLD-circuit. By employing different data-acquisition techniques such as time-series plot, phase portrait, Poincare section, spectrum density plot, and bifurcation diagram, we aim to observe the varying period of the voltage signal across the resistor. Each of these plots are an attempt to present a clear picture of bifurcation—the point where period-doubling takes place. We want to be able to distinguish higher order periods such as $8T$ from chaos via these plots.

KEYWORDS: Nonlinear Dynamics Phase Portrait Poincare Section Feigenbaum Constant
Diode Recovery Time Chaos in RLD Circuit Period Quadrupling Period Doubling Bifurcation
Chaos.

Contents

1	Introduction	3
1.1	Nonlinear Dynamics	3
1.2	Chaos	3
1.3	Different Ways to Represent Chaos	3
1.3.1	Time-Series	4
1.3.2	Phase Portrait	4
1.3.3	Poincare Section	4
1.3.4	Bifurcation Diagram	4
2	The Experiment	6
2.1	The Circuit	6
2.2	The Mathematical Model	6
2.3	The Physical Model	9
2.3.1	The diode recovery-time	9
2.3.2	The period-doubling route to chaos	9
2.4	The Procedure	10
2.4.1	The Setup	10
2.4.2	Time-series plot and Phase portraits of voltage across resistor.	11
2.4.3	Observing period bifurcations on the spectrum analyzer	13
3	Bifurcation Diagrams	16
3.1	Overview of the Process	16
3.2	Amplitude Modulation	16
3.2.1	Simple Tests for Amplitude Modulation	17
3.2.2	Amplitude Modulation for RLD-Circuit	19
3.3	Data Processing via LabVIEW	19
Bibliography		22

List of Figures

1	Different ways of representing the nonlinear behavior of a system [9]. (a) Time-series plots displaying period-doubling for the increase in γ . (b) Phase portraits displaying the change in period from two to four. (c) Poincare section showing a simplified version for the period-2 phase portrait. (d) The bifurcation diagram for the changing values of γ and the corresponding change in $\phi(t)$	5
2	(a) The experimental RLD-circuit. (b) Equivalent circuits for forward and reverse bias cycle.	6
3	Circuit current, I , and diode voltage, V_d , (period-2) [4]. The diode conducts when $V_d = -V_f$ behaving like a circuit as shown in Figure 2a. Otherwise it behaves as a capacitor.	10
4	Schematic for the circuit for measuring V_R across the resistor.	11
5	Time-series plots and phase portraits for RLD-circuit showing period-doubling, period-quadrupling, and chaos at different voltages.	12
6	Period-doubling shown using time-series plot, phase portraits, and spectrum density plots at different voltages.	15
7	Amplitude-modulation of a sine wave. (a) For $\mu = 1$, the maximum voltage is 1 V, while minimum is 0 V. (b) For $\mu = 0.75$, the maximum voltage is 890 mV, while minimum is 125 mV. (c) For $\mu = 0.5$, the maximum voltage is 755 mV, while minimum is 250 mV.	18
8	Wave modulation using a saw-tooth amplitude-modulating signal. For $\mu = 0.5$, the maximum voltage is 740 mV, while the minimum is 240 mV.	19
9	The front panel of RLD_DAQ.vi—the LabVIEW program used to store data and display it via time-series plot, phase portrait, and Poincare section.	20
10	Bifurcation diagrams: (a) without any filter. (b) with Savitzky Golay Filter fitted to 5 degree polynomial. (c) with Savitzky Golay Filter fitted to 3 degree polynomial.	21

1 Introduction

1.1 Nonlinear Dynamics

For a nonlinear systems, the change in the output parameter is not proportional to that of the input parameter. This means on increasing input, the corresponding output variable shows different behaviours—ranging from doubling of the output to four times to chaos and then back to an integer multiple of the initial value (it could be some other pattern too).

Mathematically, a nonlinear system can be described using a set of simultaneous equations in which the unknown variable is in the argument of a higher degree polynomial or a trigonometric function. For such systems, the equation(s) cannot be written as a linear combination of the unknown variables or functions that appear in them. For instance, if x is the input and y the output parameter, the principle of superposition states that:

$$y(x_1 + x_2 + \dots + x_n) = y(x_1) + y(x_2) + \dots + y(x_n) \quad (1)$$

The above mathematical expression shows that when the stimuli to a linear system is doubled, the response would also double. However, for a nonlinear system, the response can be greater or less than that.

What makes nonlinearity so important? Basically, for a linear system, the change in the input parameter doesn't change the qualitative behavior of the system. On the other hand, for nonlinear a system, a small change in input can lead to sudden and drastic changes in both the qualitative and quantitative nature of the system. If, for a given value, the behavior is be periodic. For another value—only slightly different from the rest—the behavior might become aperiodic.

1.2 Chaos

As mentioned, the output for a nonlinear system can demonstrate different behaviours for the corresponding changes in input—chaos being one of them. It refers to the aperiodic behaviour of the system, which is usually random and noisy. Chaos is identified by its hypersensitive dependence on initial conditions. A minute change in the initial conditions can lead to a drastic dynamical evolution of the system.

Generally, chaos begins with period-doubling bifurcation: system switches from period-1 to period-2 at a precise value of the input parameter (say V). With further increase in the value of V , successive bifurcations take place, which change the period from twice to four times to finally aperiodic or chaotic.

1.3 Different Ways to Represent Chaos

There are various ways to represent the data obtained from a nonlinear system. Below, we have discussed some of them as we will use them in the course of our experiment.

Following ways of representing chaos have been explained in terms of a driven damped pendulum (DDP). The differential equation for the system is,

$$\ddot{\phi} + 2\beta\dot{\phi} + \omega_o^2 \sin(\phi) = \gamma\omega_o^2 \cos(\omega t),$$

where γ is the driving force (input parameter) that is varied for each iteration.

1.3.1 Time-Series

Time plot is the simplest way to observe the nonlinear behaviour of a system. By changing the input parameter, we observe changes in the period of the system. In the case of DDP, for each values of the driving force, we can plot ϕ against time and examine the period of the pendulum. On increasing γ , we expect the period of the system to double, then three times, four times, eight times and so on till we enter the region of chaos. We can see from Figure 1a, how the increase in the value of γ from 1.06 to 1.078 causes period-doubling.

1.3.2 Phase Portrait

Another way to observe both the position, $\phi(t)$, and the angular velocity, $\dot{\phi}(t)$, of the pendulum as time evolves is via the phase portrait. In principle, if one knows $\phi(t)$ for all times, then one can calculate $\dot{\phi}(t)$ by simple differentiation.

Phase portrait are drawn by plotting the pair of values $(\phi(t), \dot{\phi}(t))$ as a point in a two-dimensional plane, where the horizontal axis labels $\phi(t)$ and the vertical axis $\dot{\phi}(t)$. The graph displays several loops, each corresponding to a particular period. If there is a single loop in the plot, it means its a period-1 wave. For two loops, period-doubling has occurred, and so on. However, if none of the loops are identical or fully overlapping then it means the system is in the chaotic region. Figure 1b shows the transition from period-2 to period-4.

1.3.3 Poincare Section

Poincare diagram is an extension to phase portrait. It is particularly useful to show the chaotic region as they are clearer and easy to understand. The basic purpose of these maps is to reduce an n -dimensional system to an $(n - 1)$ -dimension to make the analysis easier. For each complete cycle in the phase portrait, the Poincare section displays a single dot. If all the loops on the phase portrait have the same period then there is a single point in the Poincare picture. Two dots represents period-2, four dots period-4, and numerous for chaos. Figure 1c shows the phase portrait and the corresponding Poincare section for period-24.

1.3.4 Bifurcation Diagram

Lastly, the bifurcation diagram is an efficient way to see the complete picture of the varying behaviour of a nonlinear system. It is simply a plot of the changing input against the output. Each splitting in the plot indicates a change in period. For a DDP, the bifurcation diagram plots $\phi(t)$ against γ , as shown in Figure 1d. As the control parameter γ varies, the response variable $\phi(t)$ begins to bifurcate: two paths for the first bifurcation, four for the second, eight for third one, and so on. The fuzzy bands in the middle indicate chaotic behavior. One can also observe the periodic bands following the chaotic region, showing how chaos can suddenly vanish and give rise to a certain higher order period.

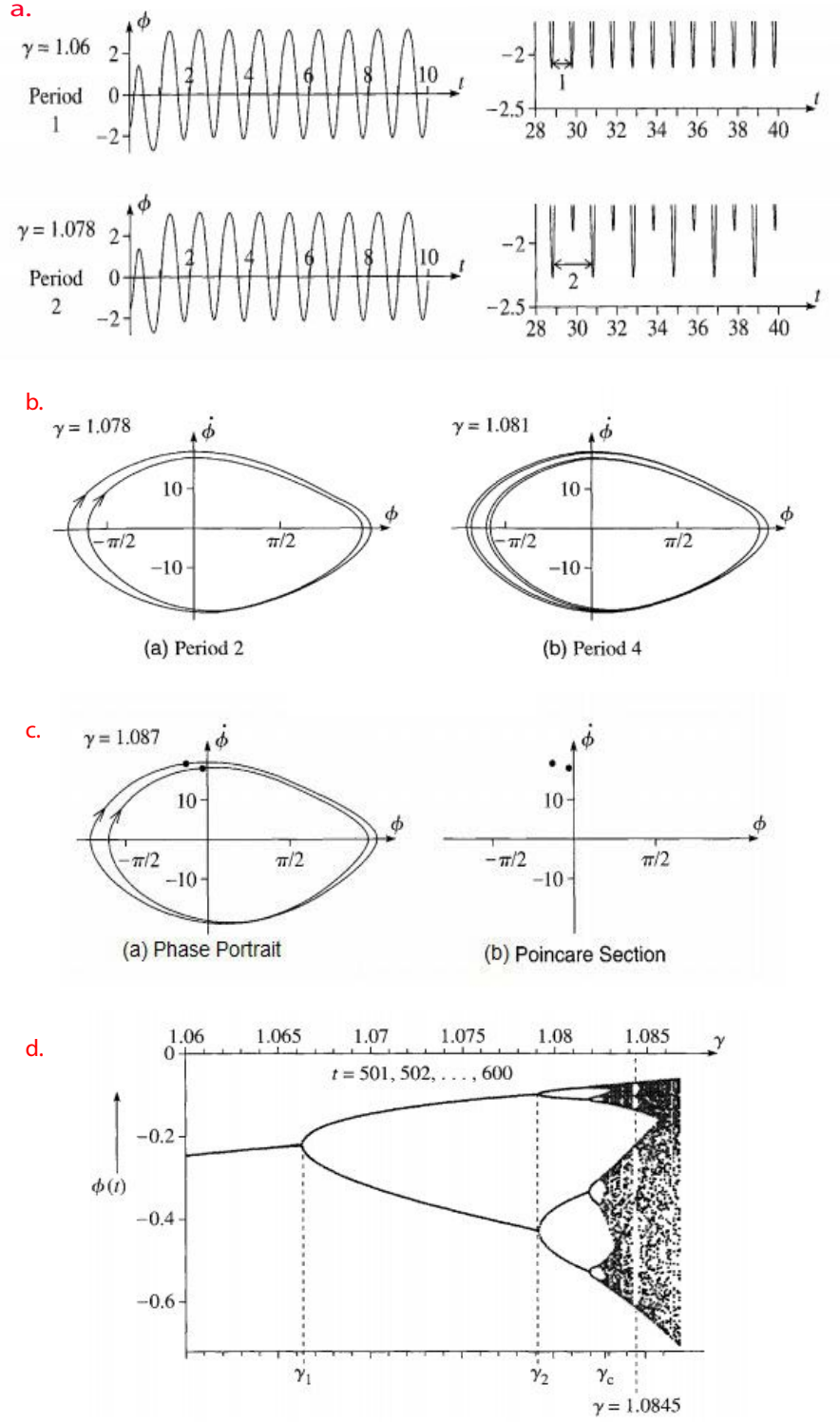


Figure 1: Different ways of representing the nonlinear behavior of a system [9]. (a) Time-series plots displaying period-doubling for the increase in γ . (b) Phase portraits displaying the change in period from two to four. (c) Poincaré section showing a simplified version for the period-2 phase portrait. (d) The bifurcation diagram for the changing values of γ and the corresponding change in $\phi(t)$.

2 The Experiment

This experiment involves an RLD-circuit that exhibits nonlinear behaviour. It is remarkable to see that how such a simple circuit can exhibit a complex behavior like chaos.

2.1 The Circuit

An RLD-circuit consists of a resistor, inductor, and a diode connected in series. What induces a nonlinear behaviour in the simple circuit is the way it behaves when subject to AC voltage. The diode in the circuit works in two modes: forward biased and reverse biased.

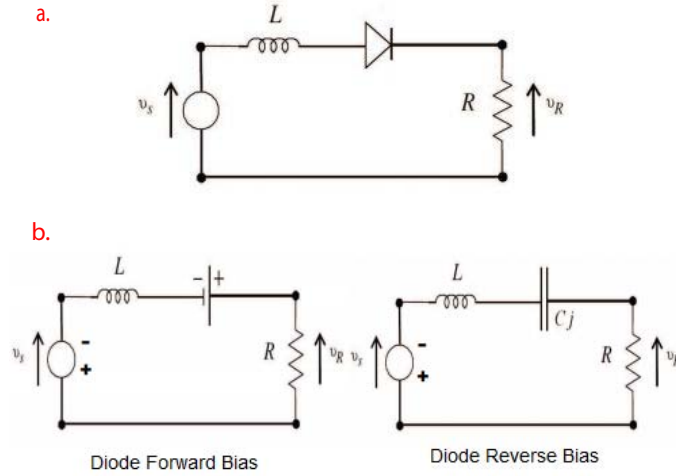


Figure 2: (a) The experimental RLD-circuit. (b) Equivalent circuits for forward and reverse bias cycle.

2.2 The Mathematical Model

When the diode is in the **forward bias mode**, the circuit is said to be in the conducting cycle. Here the circuit reduces to what is shown in Figure 2b (left side), with the diode acting as a fixed voltage drop (battery). The Kirchhoff's voltage law applied to the circuit is,

$$L \frac{dI}{dt} + RI = V_o \sin \omega t + V_f, \quad (2)$$

where V_o is the peak amplitude of the AC input voltage and V_f is the diode's forward voltage drop, which

is generally around 0.5-1.0 V. The solution to the above nonhomogeneous differential equation is,

$$\begin{aligned}\frac{dI}{dt} + \frac{RI}{L} &= 0, \\ \int \frac{1}{I} dI &= - \int \frac{R}{L} dt, \\ I_c &= -K \exp(-Rt/L),\end{aligned}\tag{3}$$

where I_c is the complementary solution. Now we will find the particular solutions to the differential equations. The guess solution for this equation is,

$$\begin{aligned}I_p &= A \sin \omega t + B \cos \omega t + C, \\ \dot{I}_p &= A\omega \cos \omega t - B\omega \sin \omega t.\end{aligned}$$

Substituting the guess solution into the differential equation gives,

$$A\omega \cos \omega t - B\omega \sin \omega t + \frac{R}{L}(A \sin \omega t + B \cos \omega t + C) = \frac{V_o}{L} \sin \omega t - \frac{V_f}{L},\tag{4}$$

$$\left(-B\omega + \frac{RA}{L}\right) \sin \omega t + \left(A\omega + \frac{RB}{L}\right) \cos \omega t + \frac{RC}{L} = \frac{V_o}{L} \sin \omega t - \frac{V_f}{L}.\tag{5}$$

Comparing the above equation with the actual differential equation yields,

$$C = \frac{V_f}{R}, \quad -B\omega + \frac{RA}{L} = \frac{V_o}{L}, \quad A\omega + \frac{RB}{L} = 0.$$

Solving the coupled equations gives,

$$A = \frac{V_o R}{R^2 + \omega^2 L^2}, \quad B = \frac{-V_o \omega L}{R^2 + \omega^2 L^2}.$$

And the particular solution becomes,

$$I_p = \frac{V_o R}{R^2 + \omega^2 L^2} \sin \omega t + \frac{-V_o \omega L}{R^2 + \omega^2 L^2} \cos \omega t + \frac{V_f}{R}.\tag{6}$$

Whereas the final solution turns out to be,

$$I(t) = \left(\frac{V_o}{Z_a}\right) \cos(\omega t - \theta) + \frac{V_f}{R} + A e^{-Rt/L},\tag{7}$$

where $\theta = \tan^{-1}(-\omega L/R)$ represents a phase delay; A is the constant of integration i.e. to be calculated using the initial conditions, and $Z_a = \sqrt{R^2 + \omega^2 L^2}$ is the forward bias impedance of the circuit.

On the other hand, for the **non-conducting cycle**, the diode behaves like a capacitor with capacitance

equal to the junction capacitance (C_j). The equivalent circuit can be represented as a driven RLC-circuit shown in Figure 2b (right side). The loop equation then becomes a second order differential equation:

$$L \frac{d^2 I}{dt^2} + R \frac{dI}{dt} + \left(\frac{1}{C_j} \right) I = V_o \omega \cos \omega t. \quad (8)$$

The solution of the equation is found by,

$$m^2 + \frac{R}{L} m + \frac{1}{LC_j} = 0,$$

$$m = \frac{-R}{2L} \pm i\omega_b,$$

where,

$$\omega_b^2 = \omega_o^2 - \left(\frac{R}{2L} \right)^2, \quad \omega_o^2 = \frac{1}{LC_j}.$$

The complementary solution then becomes,

$$I_c = B \exp\left(\frac{-Rt}{2L}\right) (\cos \omega_b t - \phi). \quad (9)$$

The guess solution for the differential equation is,

$$I_p = A \sin \omega t + B \cos \omega t, \quad \dot{I}_p = A \omega \cos \omega t - B \omega \sin \omega t, \quad \ddot{I}_p = -A \omega^2 \sin \omega t - B \omega^2 \cos \omega t.$$

Substituting the guess solution into the differential equation results in,

$$-A \omega^2 \sin \omega t - B \omega^2 \cos \omega t + \frac{R}{L} (A \omega \cos \omega t - B \omega \sin \omega t) + \omega_o^2 (A \sin \omega t + B \cos \omega t) = V_o \omega \cos \omega t, \quad (10)$$

$$\left(-A \omega^2 - \frac{RB \omega}{L} + \omega_o^2 A \right) \sin \omega t + \left(-B \omega^2 + \frac{RA \omega}{L} + B \omega_o^2 \right) \cos \omega t = V_o \omega \cos \omega t. \quad (11)$$

Comparing coefficients yields,

$$B = \left(\frac{LV_o \omega - RA \omega}{(\omega_o^2 - \omega^2)L} \right), \quad A = \frac{RV_o \omega^2 L}{L^2(\omega_o^2 - \omega^2) + R^2 \omega^2}.$$

The particular solution obtained is then,

$$I_p = \frac{V_o \omega}{L \sqrt{(\omega_o^2 - \omega^2)^2 + R \omega / L}} \cos(-\theta), \quad (12)$$

and the final solution is,

$$I(t) = \left(\frac{V_o}{Z_b} \right) \cos(\omega - \theta_b) + B e^{-Rt/2L} \cos(\omega_b t - \phi), \quad (13)$$

where $\theta_b = \frac{wR}{L(w_o^2 - w^2)}$, $Z_b = \left(\frac{L}{\omega} \right) \sqrt{(\omega_o^2 - \omega^2)^2 + \left(\frac{R\omega}{L} \right)^2}$, and B and ϕ are the constants of integration and can be found using the initial conditions. .

2.3 The Physical Model

2.3.1 The diode recovery-time

Before getting started with the experiment, we need to understand the significance of an important parameter: the diode's recovery time. It is the time taken by the diode to completely stop the flow of forward current as it moves into the non-conducting cycle. It depends on the amplitude of the forward current that has just passed through it. The greater the amplitude, the longer the diode's recovery time. Quantitatively speaking, the recovery represented as, [4]:

$$\tau_r = \tau_m [1 - \exp(-|I_m|/I_c)], \quad (14)$$

where $|I_m|$ is the amplitude of the recent most forward current, and τ_m and I_c are the fabrication parameters for a specific diode.

2.3.2 The period-doubling route to chaos

Now it is important to understand the physical description of how period-doubling is caused in an RLD-circuit. [4]. For every reverse bias cycle, a small amount of reverse current flows through the diode due to its finite recovery time. If the peak current $|I_m|$ is large in the conducting cycle (figure (3), interval 'a'), the diode switches off with a certain delay (figure (3) interval 'b'). This happens due to its finite recovery time, which allows current to flow even in the reverse-bias cycle (shown as interval 'b'). The reverse current, in turn, prevents the diode from instantly switching on in the forward bias cycle. Instead, it turns *on* with a delay (interval 'c'). This keeps the forward peak-current smaller than in the previous forward bias cycle, hence giving rise to two distinct peaks—period-doubling—in the forward current. When the drive voltage increases, period-2 bifurcation is followed by a higher degree bifurcations, which eventually leads to chaos.

Notice that it takes *two* cycles of the driving signal to observe period-doubling.

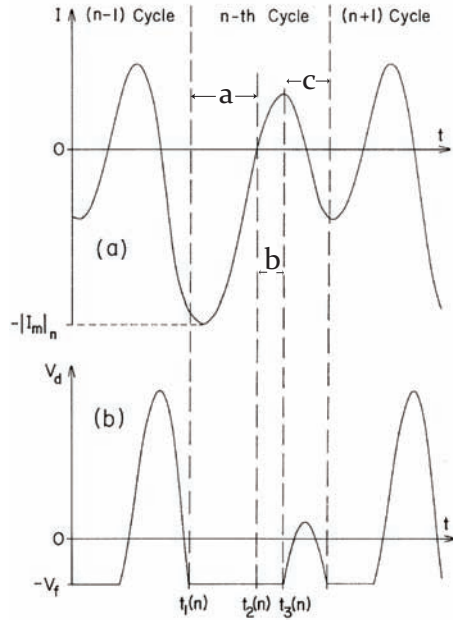


Figure 3: Circuit current, I , and diode voltage, V_d , (period-2) [4]. The diode conducts when $V_d = -V_f$ behaving like a circuit as shown in Figure 2a. Otherwise it behaves as a capacitor.

2.4 The Procedure

2.4.1 The Setup

The equipment used in the experiment are listed here,

1. Oscilloscope (Agilent DSO-X 2002A)
2. Function Generator (BK Precision 4086)
3. Data Acquisition Setup (National Instruments DAQ card)
4. Spectrum Analyser (Agilent N9320B)
5. RL-Diode circuit components - 100 Ω Resistor, ≈ 15.054 mH Inductor¹, 1N4007 Diode

¹**SIDE NOTE:** Different inductors were calibrated and their respective impedance was found to choose a suitable one for the experiment. We were looking for an inductor that could clearly exhibit the nonlinear behaviour of the diode. The inductor that we chose has inductance ≈ 15.054 mH and resistance $R_L = 6.184 \Omega$. The impedance is then:

$$\begin{aligned}
 Z &= R_L + i\omega L \\
 Z &= 6.184 + i4729.35 \\
 Z &= (4.73 \angle 90^\circ) \text{ k}\Omega
 \end{aligned}$$

Chaos is usually observed by changing only one parameter (keeping all others constant) and observing the corresponding response of the system. For RLD-circuit, we can choose from the two variable parameters: frequency and voltage. For our experiment, we kept the frequency constant at 50 kHz and varied the amplitude of the input AC signal. Also, all input voltages, V_{in} , fed into the circuit via signal generator were peak-to-peak voltages.

2.4.2 Time-series plot and Phase portraits of voltage across resistor.

We connected the circuit to the signal generator in series as shown in Figure 4. Using a BNC-to-Crocodile clip cable, the signal across the resistor, V_R , was fed into Channel 1 of the Agilent oscilloscope.

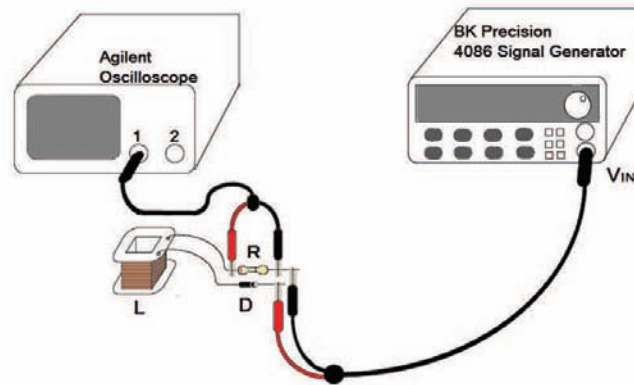


Figure 4: Schematic for the circuit for measuring V_R across the resistor.

With fixed frequency, the amplitude of the input signal, V_{in} , was increased in steps of 0.01 V. The oscilloscope scales were continuously being adjusted to view the complete waveform. When working with such a high frequency, we need to tweak the time-base setting, trigger level, and the input amplitude to be able to see a clear signal. For our case, a clear signal received at 1.6 V. For fluctuating signals, a more stable and finer waveform was obtained by increasing the number of samples (of the input signal at Channel 1) being averaged out by the oscilloscope.

Each picture on the left in Figure 5 is a time-series plot with two signals: one across the resistor (yellow waveform on the top), second across resistor+inductor (green waveform in the bottom). The pictures in the right column are the corresponding phase portraits². Figure 5 (1a) displays period-1 waveform at $V_{in} = 1.37$ V. As the voltage increases (as shown in the figure), the period to change from $T = 20 \mu s$ at $V_{in} = 3.10$ V to $T = 40 \mu s$ at $V_{in} = 3.38$ V to $T = 80.7 \mu s$ at $V_{in} = 4.26$ V and finally chaos with an aperiodic waveform at $V_{in} = 4.46$ V.

²**SIDE NOTE:** Voltage across resistor, V_R (fed into channel 1), is proportional to the rate of change of current, $\frac{dI}{dt}$, while the voltage across the complete circuit is proportional to current I (fed into channel 2). Plotting these two variables gives us the phase portraits

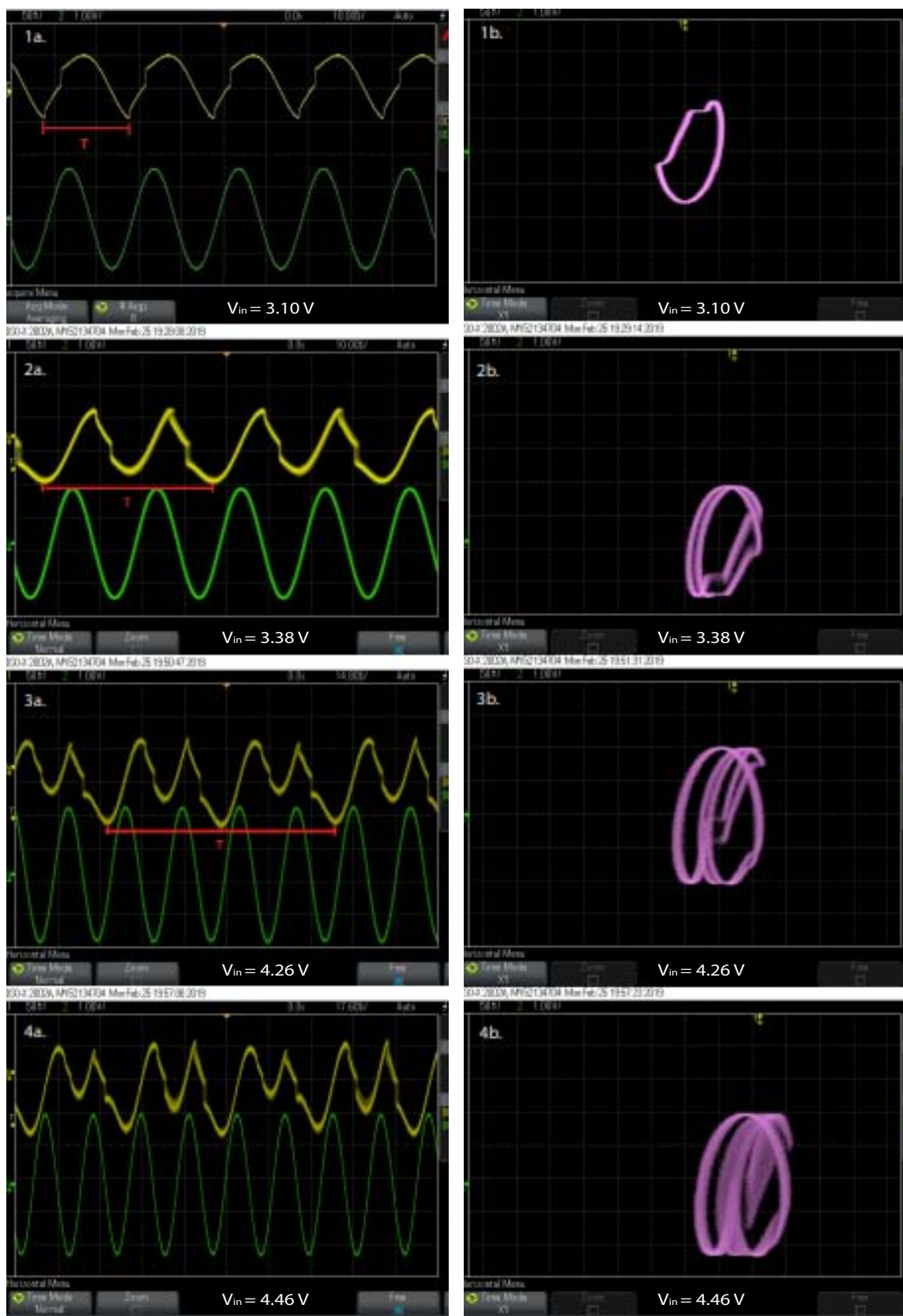


Figure 5: Time-series plots and phase portraits for RLD-circuit showing period-doubling, period-quadrupling, and chaos at different voltages.

2.4.3 Observing period bifurcations on the spectrum analyzer

In the previous section, we observed only two bifurcations—2T and 4T. This is because, it is not possible to observe the third bifurcation clearly in a time-series plot. One way to observe the third bifurcation is through the Fourier spectrum of the signal. For any given signal, its Fourier transform provides all the underlying frequencies that make up the signal. In our case, a spectrum analyzer is used to identify the different frequencies present in the signal. The number of peaks in the graph is a measure of wave's period—four peaks mean period-4.

Using theory, we can predict the value of the input voltage for the third bifurcation before hand. We can then compare the calculated value to the experimental value to see how efficient is the technique of observing bifurcation using a spectrum analyzer.

Feigenbaum noticed that *the ratio of difference of parameter values for successive bifurcations is the same for all the splittings* [2]. Mathematically speaking,

$$\delta_n = \frac{\lambda_n - \lambda_{n-1}}{\lambda_{n+1} - \lambda_n},$$

where λ_n is the parameter value at which the n 'th bifurcation occurs. Moreover, this ratio converges to a specific value called the Feigenbaum constant as n approaches infinity: $\delta \equiv \lim_{n \rightarrow \infty} \delta_n = 4.669201 \dots$. Using the data from the previous run, λ_3 for the third bifurcation turn out to be,

$$4.6692 = \frac{4.26 - 3.38}{\lambda_3 - 4.26},$$
$$\lambda_3 = 4.45 \text{ V}.$$

The circuit was set up again as shown in Figure 4. The only difference being, this time the signal across the resistor that was fed into both the oscilloscope and the spectrum analyzer. Similar to the previous case, the input voltage was increased gradually at small intervals and the corresponding spectral density graphs were observed.

At $V_{in} = 2.96 \text{ V}$, the set of data across resistor shows only a single period(1T). Corresponding to it, the spectrum analyzer displays a single peak at 50 kHz as shown in Figure 6. On increasing the input voltage, the plot on the spectrum analyzer starts to change—new peaks appearing at different frequencies, indicating a change in period. This results for the variation have been displayed in Table 1 and Figure 6.

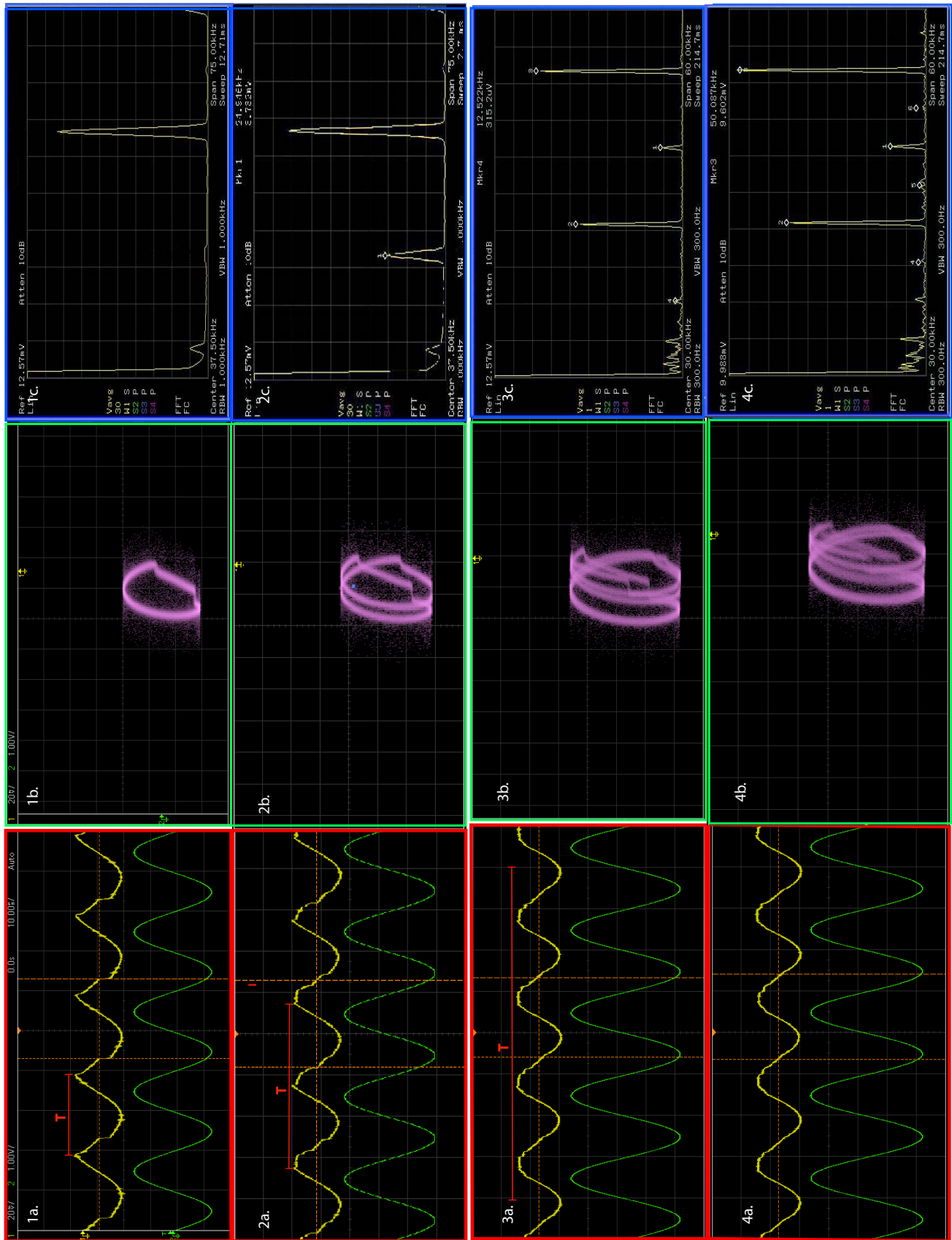
Table 1: T change in the number of peaks and their respective frequencies with the increase in the input voltage. It can be seen that as the voltage increases, the number of peaks double and so does the period of the waveform.

Voltage (V)	2.96	3.20	3.84	3.90
No. of peaks	1	2	4	8
Frequency of peaks (kHz)	50	50, 25	50, 37.5, 12, 12.5	6.3, 12.5, 18.5, 25, 31.3, 37.6, 43.8, 50
Period	1T	2T	4T	8T
Figure 6	1	2	3	4

As it can be seen from Figure 6, for each spectral density plot, the amplitude of the peaks decreases from right to left. The height of the peaks in dictates their respective contribution to the final waveform. For instance, in all plots, peak-50 kHz has the highest amplitude. This means that this frequency has contributed the most to the wave.

As we can see from Figure 6 (4), it is not easy to observe the third bifurcation (8T period) via the time-series plot and phase portraits. However, the eight distinct peaks on the spectral density plot make it convenient to spot the third bifurcation.

Experimentally, the third bifurcation occurred at $V_{in} = 3.90$ V, whereas the expected value that we calculated using the Feigenbaum constant is $V_{in} = 4.45$ V. This shows how sensitive of a phenomenon chaos is. Even with the slightest variation in the parameter, the change in the outcome can be quite drastic. And therefore, it is not easy to predict it precisely through theory.



3 Bifurcation Diagrams

3.1 Overview of the Process

The bifurcation diagram is the most efficient way to observe the nonlinear behaviour of a system. In these plots, the input voltage is varied continuously and the corresponding values for the voltage across the resistor are noted. A graph is then plotted between V_{in} (x-axis) and V_R (y-axis), which clearly displays splittings (period-doubling) of the waveform.

It is not convenient to manually increase the input voltage to record the changes in V_R . We therefore use an NI DAQ card to generate a single up-ramp voltage sweep. The signal from DAQ amplitude-modulates a 50 kHz sine wave i.e. produced by the function generator (BK 4086). The modulated signal is then fed into the circuit and a LabVIEW program is used to store the values of voltage across the resistor.

The data is received onto the computer via the oscilloscope i.e. connected to the PC via a USB port. The data recorded is used to plot phase portraits and bifurcation diagrams using LabVIEW. For phase portraits, data from channel 1 is plotted against the data from channel 2. For the bifurcation diagram, first, peaks are detected in the V_R data using LabVIEW. The sampled peak-amplitudes are then plotted against the corresponding V_{in} to produce the bifurcation graph.

3.2 Amplitude Modulation

Amplitude modulation is the technique of imprinting data onto an AC carrier waveform by changing its amplitude. In simple words, there is a message or modulating³ signal that is imprinted on a carrier signal, and the final form received is a modified, also called, a modulated signal. Mathematically speaking,

$$\text{modulating signal: } m(t) = V_m \sin w_m t, \quad (15)$$

$$\text{carrier signal: } c(t) = V_c \sin w_c t, \quad (16)$$

$$\text{modulated signal: } s(t) = V_c (1 + \mu \sin w_m t) \sin w_c t, \quad (17)$$

where μ is the modulation depth given by V_m/V_c .

From equation 17, it can be seen that the maximum for the modulated signal occurs when $\sin w_m t$ is 1, while minimum when it is -1. This results in,

$$V_{\max} = V_c (1 + \mu), \quad (18)$$

and

$$V_{\min} = V_c (1 - \mu). \quad (19)$$

³The highest frequency for the modulating signal is normally less than 10% of the carrier frequency. In our case, if the frequency of the carrier wave is 50 kHz, the maximum frequency for the modulating signal should not be over 5 kHz.

3.2.1 Simple Tests for Amplitude Modulation

After theoretically deriving the formulae for amplitude of the modulated wave, it's time to test them experimentally. The purpose is to see whether or not the formulae conform to the experiment results.

The modulating signal used was a sine wave of frequency 500 Hz and amplitude 3 V peak-to-peak, produced by DAQ. While the carrier signal was a sine wave of frequency 50 kHz and amplitude 2 V peak-to-peak produced by signal generator. The modulation depth was varied and the respective changes in the maximum and minimum voltage were recorded. The results are shown in Table 2 and Figure 7.

Table 2: V_{\max} and V_{\min} for a wave modulated using a sine wave modulation signal.

μ	V_{\max} (V)	V_{\min} (V)
1.00	1.00	0.00
0.75	0.89	0.13
0.50	0.76	0.25

Using these experimental results, a mathematical model is derived, according to which V_{\max} and V_{\min} turn out to be,

$$V_{\max} = \frac{V_c}{2} (1 + \mu), \quad (20)$$

and

$$V_{\min} = \frac{V_c}{2} (1 - \mu). \quad (21)$$

On comparing equation 20 and 21 to equation 18 and 19, one can notice the difference. The mathematical model that the signal generator BK 4086 abides to doesn't fully conform to theoretical model.⁴

Lastly, the amplitude-modulation of a sine wave of frequency 50 kHz and amplitude 2 V peak-to-peak was performed using a saw-tooth wave of frequency 500 Hz and amplitude 3 V peak-to-peak. The results obtained seemed to conform to the formulae derived experimentally. The results are shown in Table 3 and Figure 8.

Table 3: V_{\max} and V_{\min} for a wave modulated using a saw-tooth modulation signal

μ	V_{\max}/V	V_{\min}/V
1	1	0
0.75	870	120
0.5	740	240

⁴The purpose of the amplitude-modulation test is to devise a mathematical model that could be used to understand the working of signal generator and determine the amplitude of the input voltage for the ramp-up sweep.

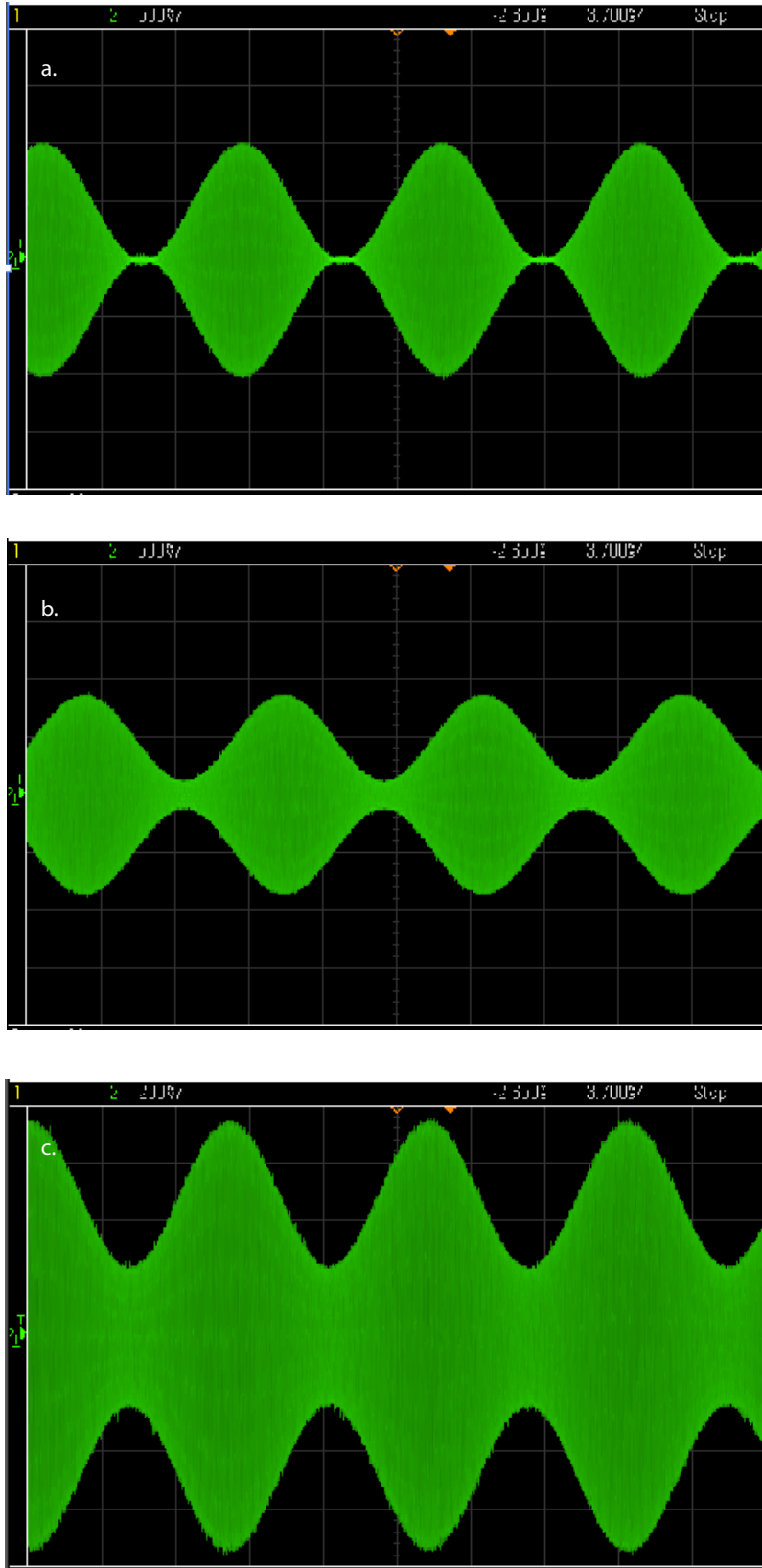


Figure 7: Amplitude-modulation of a sine wave. (a) For $\mu = 1$, the maximum voltage is 1 V, while minimum is 0 V. (b) For $\mu = 0.75$, the maximum voltage is 890 mV, while minimum is 125 mV. (c) For $\mu = 0.5$, the maximum voltage is 755 mV, while minimum is 250 mV.

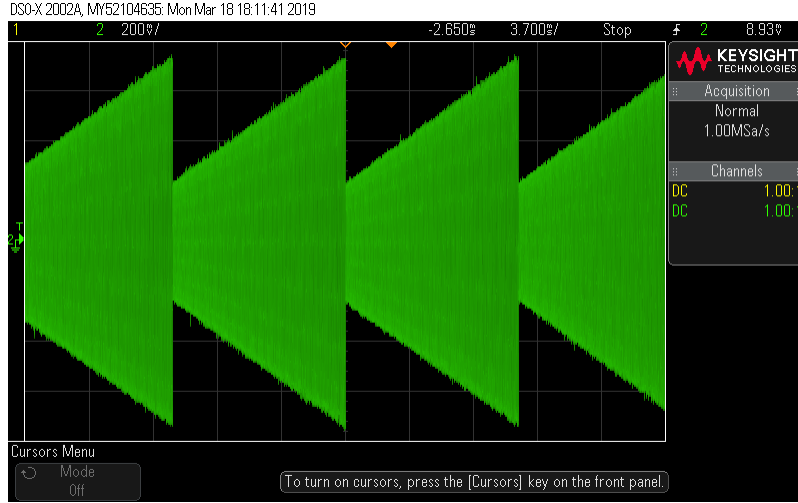


Figure 8: Wave modulation using a saw-tooth amplitude-modulating signal. For $\mu = 0.5$, the maximum voltage is 740 mV, while the minimum is 240 mV.

3.2.2 Amplitude Modulation for RLD-Circuit

In order to produce the bifurcation diagram, we need an up-ramp signal of amplitude 10 V. This would be the modulated signal running through the circuit. To produce it, DAQ generates a modulating signal of frequency 1 kHz and amplitude 1.5 V. The total time period of the signal is 70 s, in which the ramp begins after 50 s.

Using equation 20, we first find the amplitude for the carrier wave—one that results in a 10 V ramp of modulated signal. Given the modulation depth, μ , is 1, V_{\max} turns out to be,

$$V_{\max} = \frac{V_c}{2} (1 + \mu)$$

$$V_c = 10 \text{ V}$$

3.3 Data Processing via LabVIEW

After developing the modulation mechanism that sends a ramp signal of increasing voltage into the circuit, the next step is data acquisition and processing. For this purpose, we have three separate LabVIEW files whose details and functions are listed in Table 4.

Table 4: LabVIEW files used for creating the bifurcation diagram.

Filename	Functions
RLD_DAQ.vi	It generates a amplitude-modulation ramp that is fed into the circuit. Once the signal starts appearing clearly on the oscilloscope, which takes around 40 seconds, the LabVIEW file starts recording two sets of data ⁵ : one across the resistor (V_R) and the other across the resistor + inductor (V_{R+L}) and stores them in separate files. Using this data and a peak detection algorithm, it then creates time-series plots, phase portraits and Poincare maps. Figure 9 shows its front panel.
Data_Acquisition.vi	By storing voltage across resistor, it create a file of V_R with corresponding V_{in} values. This is extremely important as the bifurcation diagram is essentially a plot between these two parameters. It might seem that these two sets of data should automatically be stored side by side. However, V_{in} is the input signal whereas V_R is the output signal so a mechanism is needed to store the two together. There is also Savitzky Golay Filter to fit the data onto a polynomial of choice and minimize noise. There is a button in the front panel to control the filter and the degree of polynomial.
Peak_Detection.vi	It reads the output file from Data_Acquisition.vi and goes through all its data points to search for turning points. Finally, it note downs the value of V_R at a turning point and its respective V_{in} in a new notepad file.

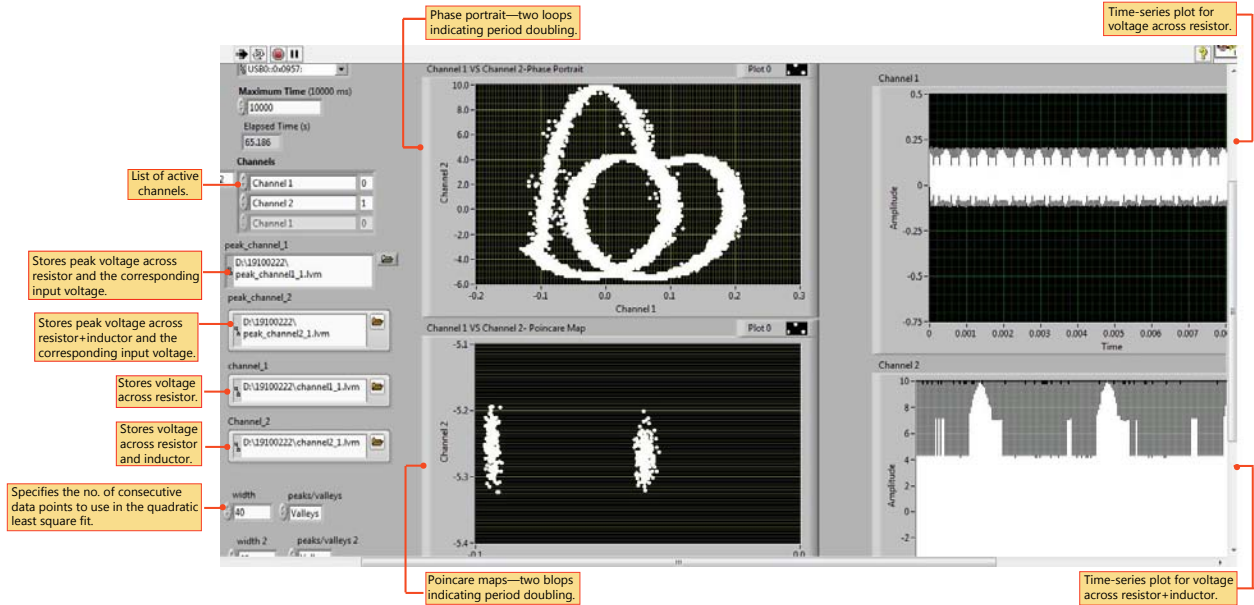


Figure 9: The front panel of RLD_DAQ.vi—the LabVIEW program used to store data and display it via time-series plot, phase portrait, and Poincare section.

The last step of the process is to plot the two columns of the output file from Peak_Detection.vi in matlab. For RLD-circuit, the bifurcation diagram is a plot of V_{in} against V_R . Some of these plots have been displayed in the figures below.

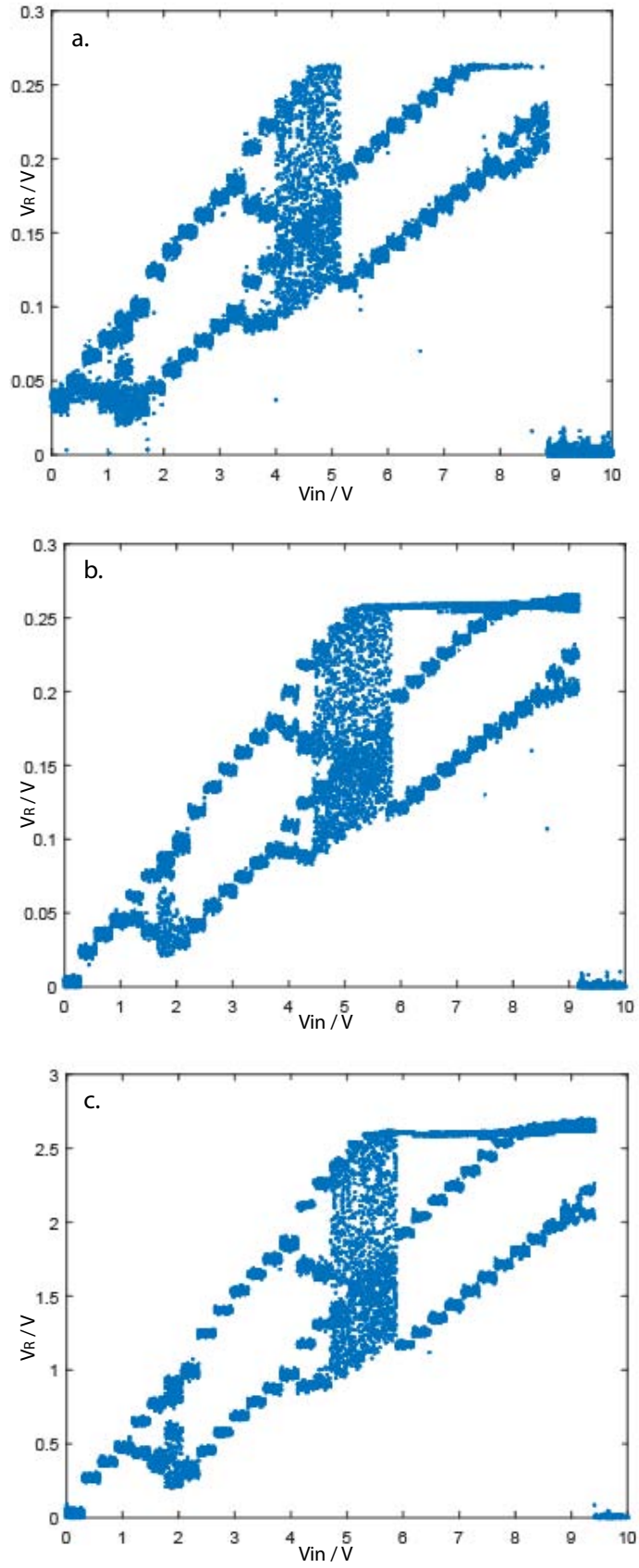


Figure 10: Bifurcation diagrams: (a) without any filter. (b) with Savitzky Golay Filter fitted to 5 degree polynomial. (c) with Savitzky Golay Filter fitted to 3 degree polynomial.

References

- [1] Gregory L. Baker, J. P. Gollub, "Chaotic dynamics: an introduction", 2nd Edition, Melbourne: Cambridge University Press, 1996, Ch. 1-4.
- [2] Robert C. Hilborn, "Chaos and Non-Linear Dynamics: An Introduction for Scientists and Engineers", 2nd Edition, NewYork: Oxford University Press, 2000, Ch. 1-4.
- [3] J. Testa, J Perez and C. Jefferies, "Evidence for Universal Chaotic Behavior of a Driven oscillator", Phys. Rev. Lett., Vol. 48, pp. 714-717, 1982.
- [4] R.W. Rollins and E. R. Hunt, "Exactly Solvable Model of a Physical System Exhibiting Universal Chaotic Behavior", Phys. Rev. Lett., vol. 49, pp. 1295-1298, 1982.
- [5] A. Azzouz, R. Duhr and M. Hasler, "Transition to Chaos in a Simple Nonlinear Circuit Driven by a Sinusoidal Voltage Source", IEEE Trans. Circuits Syst., Vol. CAS-30 (12), 1983.
- [6] M. P. Hantias, Z. Avgerinos, G.S. Tombras, "Period Doubling, Feigenbaum constant and time series prediction in an experimental chaotic RLD circuit", Chaos, Solitons and Fractals 40 (2009); 1050-1059.
- [7] A.B. Ozer, E. Akin, "Tools for Detecting Chaos", SAÜ Fen Bilimleri Enstitüsü Dergisi 9. Cilt, 1. Say 2005.
- [8] N. C. Ropes, "Poincare Sections and the R-L-Diode Circuit", 28th Southeastern Symposium on System Theory (SSST), 1996.
- [9] John. R. Taylor, "Classical Mechanics", University Science Books, 2005.